

TRPV2 channel inhibitors attenuate fibroblast differentiation and contraction mediated by keratinocyte-derived TGF- β 1 in a wound healing model using rat skin

Taro Ishii¹), Kunitoshi Uchida²), Shozaburo Hata¹), Mitsutoki Hatta²), Tomo Kita²), Yuki Miyake¹), Kazuhiko Okamura³), Sachio Tamaoki¹), Hiroyuki Ishikawa¹), Jun Yamazaki²)

Departments of ¹) Oral Growth & Development, ²) Physiological Science & Molecular Biology, and ³) Morphological Biology, Fukuoka Dental College

Corresponding author: Jun Yamazaki, PhD

Department of Physiological Science & Molecular Biology, Fukuoka Dental College

2-15-1 Tamura, Sawara-ku, Fukuoka 814-0193, Japan

Tel.: 81-92-801-0411 ext 669; Fax: 81-92-801-4909; E-mail: junyama@college.fdcnet.ac.jp

Running title: TRPV2- and keratinocyte-mediated wound contraction

Keywords: keratinocyte, fibroblast, transforming growth factor- β 1, TRPV2

Conflicts of Interest: The authors have no conflict of interest to declare.

Text, 6173 words (excluding title and reference pages); number of references, 49;

number of figures, 8; supplemental material, 1; supplemental figures, 5

Funding sources:

JSPS KAKENHI (Grant-in-Aid for Scientific Research, Grant Nos. JP15K11358 and JP16K20662) and MEXT KAKENHI (Grant-in-Aid for Scientific Research on Innovative Areas [Thermal Biology], Grant No. JP15H05298).

Abstract

Background: Keratinocytes release several factors that are involved in wound contracture and scar formation. We previously reported that a three-dimensional reconstruction model derived from rat skin represents a good wound healing model.

Objective: We characterized the role of transient receptor potential (TRP) channels in the release of transforming growth factor (TGF)- β 1 from keratinocytes and the differentiation of fibroblasts to identify possible promising pharmacological approaches to prevent scar formation and contractures.

Methods: The three-dimensional culture model was made from rat keratinocytes seeded on a collagen gel in which dermal fibroblasts had been embedded.

Results: Among the TRP channel inhibitors tested, the TRPV2 inhibitors SKF96365 and tranilast attenuated most potently keratinocyte-dependent and -independent collagen gel contraction due to TGF- β signaling as well as TGF- β 1 release from keratinocytes and α -smooth muscle actin production in myofibroblasts. Besides the low amounts detected in normal dermis, TRPV2 mRNA and protein levels were increased after fibroblasts were embedded in the gel. TRPV2 was also expressed in the epidermis and keratinocyte layers of the model. Both inhibitors and TRPV2 siRNA attenuated the intracellular increase of Ca²⁺ induced by the TRPV agonist 2-aminoethoxydiphenyl borate in TGF- β 1-pretreated fibroblasts.

Conclusion: This is the first study to show that compounds targeting TRPV2 channels ameliorate hypertrophic wound contraction through the inhibition of TGF- β 1 release and the differentiation of dermal fibroblasts.

1. Introduction

The wound healing process in skin proceeds sequentially in three phases, namely, inflammation, proliferation, and scar maturation, and involves sequential interactions of different cell types [1]. In granulation tissue, fibroblasts called myofibroblasts [1,2] obtain a contractile phenotype through the expression of α -smooth muscle actin (α -SMA) [3,4]. Such differentiation of dermal fibroblasts is believed to be involved in pathogenic scarring and fibrosis [5]. Thus, pharmacological intervention in the differentiation of fibroblasts may be beneficial for the prevention of hypertrophic scar formation and contractures.

Keratinocytes at the wound edge migrate over granulation tissue and then produce new stratified layers (re-epithelialization) through the production of many growth factors and cytokines, including transforming growth factor (TGF)- β s. TGF- β s are secreted by platelets, fibroblasts, macrophages, and keratinocytes within injured tissue and stimulate granulation tissue formation and myofibroblast production [2,6-8]. Previously, we demonstrated that keratinocytes secrete the latent form of TGF- β 1, which upregulates the expression of α -SMA in fibroblasts after the activation of latent TGF- β 1 [9]. Thus, we proposed that inhibitors of metalloproteinases and integrin α v, which have a role in the activation of TGF- β 1, could be therapeutic targets for the prevention of hypertrophic scar formation.

Possible other approaches are to target the different ion channels underlying hypertrophic scar formation. Accumulating evidence suggests that the activation of transient receptor potential (TRP) channels, which are nonselective ion channels, contributes to wound healing responses. In corneal fibroblasts, TGF- β 1-induced myofibroblast development is highly dependent on TRPV1 [10]. TRPV4 is required for

the TGF- β 1-induced differentiation of cardiac fibroblasts into myofibroblasts [11]. TRPV4 activity results in the differentiation of lung myofibroblasts and pulmonary fibrogenesis through the TGF- β 1 signaling pathway [12]. TRPA1 is required for TGF- β 1 signaling and post-alkali burn inflammation and fibrosis in mouse corneal stroma [13]. TRPC3 is highly expressed in human hypertrophic scar tissue and its overexpression promotes wound constriction [14]. TRPC6-mediated Ca²⁺ influx and calcineurin activity are required for myofibroblast transdifferentiation and wound healing [15]. TRPC6 facilitates stress fiber formation, and its inhibition suppresses TGF- β 1-mediated excessive intestinal fibrosis [16]. TRPM7 is a major Ca²⁺-permeable channel with an essential role in TGF- β 1-elicited fibrogenesis in human atrial fibrillation [17]. All of these studies focused on the roles of ion channels and downstream intracellular signaling pathways in fibroblast differentiation, although it remains uncertain whether the ion channel-mediated wound healing process is based on interactions between keratinocytes and fibroblasts during re-epithelialization, where keratinocytes migrate over the damaged area of the skin.

Keratinocytes are considered to affect the expression of several factors involved in wound contracture and skin homeostasis. For instance, TRPV3 is involved in epidermal wound healing [18], while TRPV4 contributes to epidermal barrier function [19]. The use of skin equivalents effectively enables the expression of growth factors and interactions between keratinocytes and fibroblasts [20]. We previously reported that a three-dimensional (3D) reconstruction model consisting of keratinocytes and fibroblasts/myofibroblasts derived from rat skin represents a good wound healing model [9]. Animal models have attempted to reflect human wound healing impairment, such as scarring, yet there seems to be considerable differences in wound contraction among

species. In rat or mouse models, rapid wound contraction is observed predominantly, leading to wound contracture associated with the differentiation of myofibroblasts [21]. The present *in vitro* rat model, which can be generated in a short period of time, can offer reproducibility and quantified interpretation of wound contraction. Furthermore, this model can be used to clarify the interactions between keratinocytes and fibroblasts/myofibroblasts, and effectively removes the influence of complicated inflammatory processes. Using such a model, we aimed to demonstrate the mechanism underlying the release of TGF- β 1 from keratinocytes and the contraction of myofibroblasts to obtain possible promising pharmacological approaches to prevent scar formation and contractures.

We found that the TRPV2 channel inhibitors SKF96365 [22] and tranilast [23-25] were effective at inhibiting the differentiation of dermal fibroblasts and contraction. Tranilast has been used clinically for the prevention of hypertrophic scar formation in Japan [26,27]. The TRPV2 channel functions as a noxious heat sensor that can be activated by high temperature with a threshold above 52°C and has relatively high Ca²⁺ permeability [28]. TRPV2 was shown to be expressed not only in sensory neurons but also in non-neuronal tissues, suggesting its involvement in many physiological inputs besides nociception, such as mechanosensing and lipid sensing [29-31]. This is the first study to show that compounds targeting TRPV2 channels ameliorate hypertrophic wound contraction during TGF- β 1 release and α -SMA production in a culture model.

2. Materials and Methods

2.1. Antibodies and reagents

The following primary antibodies were used: mouse monoclonal anti- α -SMA (clone 1A4; Dako, Glostrup, Denmark) and rabbit polyclonal anti-TRPV2 (generously gifted by Dr. Tominaga, National Institute for Physiological Sciences, Okazaki, Japan). Recombinant human TGF- β 1 was purchased from PeproTech (Rocky Hill, NJ). LY364947 (Cayman Chemical, Ann Arbor, MI) and other water-insoluble compounds were dissolved in dimethyl sulfoxide to make stock solutions that were diluted more than 1,000-fold before use. TRP channel inhibitors and activators were purchased from commercial sources: SKF96365, AMG9810, and HC067047 (Wako Pure Chemical Industries Ltd., Tokyo, Japan), tranilast (Tokyo Chemical Industry Co., Tokyo, Japan), and 2-aminoethoxydiphenyl borate (2-APB), capsaicin, GSK1016790A, and RN1734 (Sigma-Aldrich Co., St. Louis, MO). The other compounds were obtained from Wako Pure Chemicals.

2.2. Dissociation of keratinocytes and dermal fibroblasts

Dorsal skin was obtained from 2-day-old Wistar rats; permission for the procedures used was granted by the Animal Research Committee of Fukuoka Dental College. The skin was incubated overnight at 4°C in modified Eagle's medium containing dispase (Godo Shusei, Tokyo, Japan). To obtain keratinocytes, epidermal tissue was digested at 37°C for 1 min in phosphate-buffered saline containing a 0.1% trypsin solution and 0.65 mM ethylene diamine tetraacetic acid (Gibco Life Technologies, Carlsbad, CA). Fetal bovine serum (FBS) was added to the suspension, which was then filtered (Cell Strainer; Becton Dickinson, Franklin Lakes, NJ) and resuspended in Ham's F-12

medium (Gibco), before use in the reconstruction culture.

Dermal tissue was minced into pieces and cultured in Dulbecco's modified Eagle's medium (DMEM) containing 15% FBS. Fibroblasts that sprouted from the tissue were detached and cultured in new medium containing 10% FBS for 5–6 days. Collagen gels were prepared on ice by mixing type-I collagen (0.725 volume; Nitta Gelatin, Osaka, Japan) with a reconstitution buffer (0.1 volume; 2.2 g NaHCO₃ and 4.77 g HEPES in 100 mL of a 50 mmol/L NaOH solution, pH 7.0), 5-times concentrated DMEM (0.15 volume), and 10-times concentrated Ham's F-12 medium (0.025 volume). The gel (2.5 mL) was mixed with 2.0×10^6 or 4.0×10^5 dermal fibroblasts and poured into a 2.4-cm-diameter culture insert (Millicell CM culture plate inserts; Millipore Corp., Temecula, CA) or 1.05-cm-diameter culture insert (Falcon cell culture inserts; Corning, Inc., Corning, NY), respectively. The gel was solidified by warming at 37°C. A culture insert without fibroblasts was also prepared.

2.3. Construction of the rat skin model using collagen gel matrix culture

Keratinocytes were overlaid on a collagen gel containing dermal fibroblasts that had been prepared 2 days earlier (KC[+]) (day 0, Fig. 1A). A fibroblast-embedded collagen gel without keratinocytes was also prepared (KC[-]). The culture insert was placed in an outer dish containing DMEM and Ham's F-12 medium (3:1 volume) supplemented with 10% FBS and a growth factor cocktail (0.4% v/v bovine pituitary extract, 0.2 ng/mL human epidermal growth factor, 5 µg/mL transferrin, 5 µg/mL insulin, and 0.18 µg/mL hydrocortisone; HKGS Kit; Gibco), 250 µM ascorbic acid (Sigma-Aldrich Co.), and 20 µM phosphorylethanolamine (Sigma-Aldrich Co.), and incubated at 37°C in 5% CO₂.

After the epithelial cells grew to confluency, the gel surface was transferred to an air-liquid interface by removing the inner medium and reducing the amount of the outer medium to a level that would avoid immersing or drying the surface of the gel (air-lift) (day 1, Fig. 1A). Relative gel size at each time point is expressed as % of the initial gel size, which was obtained by dividing the area of the gel by the effective membrane area of the culture insert (days 1, 4, 6, 8, and 10, Fig. 1A).

2.4. Immunohistochemical examination of the reconstructed model

The *in vivo* rat tissues or reconstructed model were fixed briefly with a 4% paraformaldehyde solution, dehydrated gradually with a 10%, 15%, and 20% sucrose solution overnight, and embedded in Super Cryoembedding Medium (Section-Lab Co., Hiroshima, Japan) for cryostat sectioning. Ten-micrometer-thick sections were incubated in 10% normal goat serum and then incubated with anti-TRPV2 (1:200) and anti- α -SMA (1:400) antibodies for 2 h, followed by a 1-h incubation with the corresponding secondary antibodies conjugated with Alexa Fluor 488 or Alexa Fluor 594 (1:800) at room temperature. The sections were counterstained with 4',6-diamidino-2-phenylindole (DAPI; ProLong Gold; Thermo Fisher Scientific, Waltham, MA). Fluorescence was observed using a confocal microscope (LSM710; Carl Zeiss MicroImaging GmbH, Jena, Germany). ZEN 2009 Light Edition (Carl Zeiss) was used for image processing.

2.5. Real-time PCR measurement of mRNA levels

Total RNA was isolated from the keratinocytes and fibroblasts/myofibroblasts in the 3D reconstruction model or from rat dorsal skin, and mRNA was

reverse-transcribed into cDNA (NucleoSpin RNA Kit; Macherey-Nagel, Düren, Germany). Quantitative PCR was performed on the samples in duplicate using a CFX96 Real-time PCR System (Bio-Rad Laboratories, Inc., Hercules, CA) with TB Green Premix Ex Taq II (Takara Bio, Shiga, Japan) and a pair of specific primers to target rat α -SMA (forward: 5'-ACTGGGACGACATGGAAAAG-3', reverse: 5'-CATACATGGCAGGGACATTG-3', GenBank accession number: NM_001613.3), TRPV2 (forward: 5'-GCTGGCTGAACCTGCTTTAC-3', reverse: 5'-CTACAGCAAAGCCGAAAAGG-3', NM_017207.3), TRPV3 (forward: 5'-AGTGCCTCTCTGGCAACTGT-3', reverse: 5'-CTGCCTCTGTTCTTCCTTGG-3', NM_145099.2), TRPV4 (forward: 5'-AGCAACCTGGAGACTGTGCT-3', reverse: 5'-TTGAACTTGCGAGACAGGTG-3', NM_023970.1), and an endogenous control, glyceraldehyde-3-phosphate dehydrogenase (GAPDH, forward: 5'-GACATGCCGCCTGGAGAAAC-3', reverse: 5'-AGCCCAGGATGCCCTTTAGT-3', NM_017008.4) under the following thermal cycling conditions: 95°C for 30 s, followed by 40 cycles of 95°C for 5 s and 60°C for 30 s. A standard curve was used to calculate the expression of TRP channels and α -SMA normalized to the endogenous control GAPDH.

2.6. Immunosorbent assay for the quantification of TGF- β 1 concentration

For quantification of the amount of TGF- β 1 released from keratinocytes, an enzyme-linked immunosorbent assay (ELISA) was performed (Quantikine; R&D Systems, Minneapolis, MN) using a collagen gel that was overlaid with keratinocytes, but not embedded with fibroblasts. At 3 days after air-lift, the culture inserts were placed in an outer dish (60-mm diameter) containing 6 mL serum-free DMEM and Ham's F-12 medium (3:1 volume) supplemented with the growth factor cocktail. The

culture supernatant was collected at days 3–7. To change the latent form of TGF- β 1 into its immunoreactive active form, the culture supernatant was treated with 1 mol/L HCl and pH was neutralized with NaOH. Optical density was measured in duplicate using a microplate reader (1420 ARVO MX; PerkinElmer, Inc., Waltham, MA). On the basis of the regression curve constructed in each experiment using the standards, the concentration of TGF- β 1 in the culture supernatant was estimated.

2.7. Ca²⁺ measurements by fluorescence imaging

Cells plated on glass coverslips were incubated with Fluo-4 acetoxymethyl ester (AM) (Invitrogen, Thermo Fisher Scientific) for 45 min at 37°C in the dark. The coverslips were transferred to a recording chamber mounted on the stage of an inverted fluorescence microscope (IX-71-FL; Olympus, Tokyo, Japan) equipped with a cooled CCD camera (CoolSNAP ES Monochrome Camera; Photometrics, Tucson, AZ). Fluo-4 was excited at 470–495 nm and the emitted fluorescence was collected through a 510–550 nm band-pass filter. Fluorescence images of more than 30 cells were captured every 3 s at room temperature using the acquisition software NIS-Elements ver. 4.50 (Nikon, Tokyo, Japan). The mean value of fluorescence intensity at 3 consecutive time points obtained from the cells in each image was calculated using ImageJ 1.47v software (National Institutes of Health, Bethesda, MD). Relative intensity was expressed as the value normalized with the maximal effect of the Ca²⁺ ionophore ionomycin (5 μ M).

For a TRPV2 silencing study with small interfering RNA (siRNA), dermal fibroblasts were seeded on coverslips in 6-well plates and transiently transfected with a mixture containing 75 pmol TRPV2 siRNA (Stealth RNAi siRNA duplex; Invitrogen)

and Lipofectamine RNAiMAX reagent (Invitrogen) in Opti-MEM medium. The following siRNA duplexes were used: 5'-GCGCUUCAUGGAGACUGAAUGGUAC-3' and 5'-GUACCAUUCAGUCUCCAUGAAGCGC-3' (siRNA #1) and 5'-AGGAACUGACUGGACUGCUAGAAUA-3' and 5'-UAUUCUAGCAGUCCAGUCAGUCCU-3' (siRNA #2). As a control, an siRNA control sequence with medium guanine-cytosine content was used (Invitrogen). Ca²⁺ imaging and real-time RT-PCR studies were performed at 2 days after transfection.

2.8. Statistical analysis

Dose-response data were fitted to sigmoidal curves to obtain IC₅₀ and hill slope values using Origin data analysis software (OriginLab Corp., Northampton, MA). All values are presented as the mean ± standard error of the mean (n, number of observations). Statistical analysis was performed using an unpaired *t*-test when 2 groups were to be compared or using one-way analysis of variance followed by Bonferroni's *post-hoc* test for the comparison of more than 3 groups. A *P*-value less than 0.05 was considered statistically significant.

3. Results

3.1. Effects of stratified keratinocytes and TGF- β signaling on the contraction of collagen gel with embedded dermal fibroblasts

In the 3D skin equivalent model (KC[+]), keratinocyte layers were shown to be differentiated after 9 days by detecting cytokeratin 10 in the outer layers (Suppl. Fig. 1). The collagen gel started to shrink within 1 day of seeding the keratinocytes, and the area gradually reached 40% of its initial size over the next 9 days (Fig. 1B). Keratinocytes seeded on the gel in the absence of fibroblasts hardly altered the size of the gel for 10 days. In the presence of LY364947 (3 μ M), an inhibitor of TGF type I receptors, the decrease in the size of the gel (gel contraction) was inhibited by 10% in the KC(+) model, suggesting the partial involvement of TGF- β signaling in gel contraction (Fig. 1C). The exogenous application of TGF- β 1 (40 ng/mL) did not cause further gel contraction. In contrast, in the model without keratinocytes (KC[-]), the collagen gel reached only 60% of its original size after 10 days (Fig. 1B). The application of LY364947 remarkably decreased this contraction. TGF- β 1 significantly increased the reduction of gel size to a level that was comparable with the maximal contraction observed in the KC(+) model (broken line, Fig. 1C). These observations suggest that keratinocyte-independent gel contraction is moderate and mediated mostly by TGF- β signaling, while stratified keratinocytes accelerate gel contraction to a similar degree as TGF- β 1-induced contraction in this model.

3.2. Involvement of TRPV channels in the contraction of collagen gel with embedded dermal fibroblasts in the presence or absence of keratinocytes

SKF96365 (50 μ M), an inhibitor of TRPV2 [31,32], inhibited gel contraction in the

KC(+) and KC(-) models (Fig. 2). This compound exerted a substantial inhibitory action in the KC(-) model during the entire time course of the experiment (Fig. 2A). In contrast, it only demonstrated a partial action in the KC(+) model; it significantly inhibited contraction after 10 days (Fig. 2B), although it barely changed the initial contraction. Such actions of SKF96365 were similar to those of LY364947. Other TRP inhibitors and activators at concentrations that have been reported to be effective, such as the TRPV1–3 activator 2-APB (100 μ M) [33,34], TRPV1 activator capsaicin (100 nM) [35], TRPV4 activator GSK1016790A (25 nM) [36,37], TRPV1 inhibitor AMG9810 (10 μ M) [32], and TRPV4 inhibitors RN1734 (10 μ M) [38] and HC067047 (1 μ M) [36,39], exhibited smaller actions. A cell viability assay revealed that these compounds did not significantly alter the viability index of dermal fibroblasts to account for their action on gel contraction (Suppl. Fig. 2).

3.3. Inhibition of gel contraction, α -SMA production, and TGF- β 1 secretion by SKF96365 and tranilast

Tranilast has been used clinically for the prevention of hypertrophic scar formation [27]. This compound was reported to inhibit TRPV2 channels [24,39]. Here, we tested the effects of SKF96365 and tranilast on fibroblast differentiation and contraction of the KC(+) model. Treatment with SKF96365 (30 μ M) and tranilast (30 μ M) restored the gel to 65–75% of its original size at 10 days after the keratinocytes were seeded (Fig. 3A, Suppl. Fig. 3). Both compounds caused concentration-dependent inhibition of collagen contraction (SKF96365, $IC_{50} = 19.6 \pm 0.7 \mu$ M, $n = 3$; tranilast, $IC_{50} = 17.7 \pm 1.6 \mu$ M, $n = 3$) (Fig. 3B). In addition, SKF96365 and tranilast attenuated the mRNA levels of the myofibroblast marker α -SMA in the collagen gel in a concentration-dependent manner,

which was consistent with the degree of gel contraction (Fig. 3C). These results suggest that these TRPV2 inhibitors attenuated the formation of myofibroblasts, resulting in the inhibition of gel contraction. This notion was supported by a partial reduction of gel contraction by TRPV2 silencing in fibroblasts using siRNA (Suppl. Fig. 4).

Next, we measured the total (active and latent) concentration of TGF- β 1 by means of an ELISA using supernatant collected from the stratified KC culture without fibroblasts, as reported previously [9]. The cells were starved of serum on day 3. For 4 days after serum starvation (days 3–7), approximately 2.4 ng/well TGF- β 1 was released from the KC culture supernatant. SKF96365 (50 μ M) or tranilast (30 μ M) significantly attenuated TGF- β 1 production (Fig. 3D). These observations suggest that TGF- β 1 was secreted from the stratified keratinocytes through the activation of SKF96365- or tranilast-sensitive ion channels, especially in the late phase of contraction in this model.

To clarify the involvement of the TGF- β pathway in SKF96365- or tranilast-sensitive gel contraction, we tested the actions of SKF96365 or tranilast on the gel size of the KC(-) model, which was contracted maximally by treatment with exogenous TGF- β 1. SKF96365 (50 μ M) and tranilast (30 μ M) indeed restored the gel by 20–30% of its initial size and significantly inhibited TGF- β 1-induced contraction on day 10 (Fig. 4). Conversely, LY364947 (3 μ M) significantly attenuated gel contraction through the blockade of TGF- β signaling. This compound had no further effect on the contraction that occurred in the presence of SKF96365 or tranilast. This observation suggests that SKF96365- or tranilast-sensitive gel contraction is mostly dependent on the TGF- β pathway.

3.4. Time-dependent expression of TRPV2 channels and α -SMA during fibroblast

differentiation

To investigate the time course of fibroblast differentiation and the expression of TRPV channels during the construction of the 3D model, we conducted real-time PCR measurements of fibroblasts and keratinocytes using specific primers for rat α -SMA and TRPV2, TRPV3, and TRPV4 channels. The mRNA level of the myofibroblast marker α -SMA was low in both the dermis and epidermis of skin from 2-day-old rats (Fig. 5). After the fibroblasts were embedded in the gel and keratinocytes were seeded, the mRNA level of α -SMA in fibroblasts was increased on days 5–9, while little change was found in its expression in keratinocytes during this period. Although TRPV2 and TRPV3 mRNA was detected at low levels in normal dermis, their expression was drastically increased at 5–7 days after the fibroblasts were isolated and embedded in the gel. TRPV4 mRNA was expressed at a relatively high level in normal dermis, but it was decreased at 5–9 days after the fibroblasts were embedded. In contrast, TRPV2 mRNA level was low in normal epidermis, but it was slightly increased at 5–9 days in keratinocytes (Fig. 5). TRPV3 and TRPV4 mRNA levels did not exhibit any obvious time-dependent changes during the construction of the 3D model.

An immunofluorescence study revealed that TRPV2 was localized in the lower epidermal layers, but not in the dermis of 2 day-old rats (Fig. 6). Immunostaining was entirely negative for α -SMA. In the model at 5 days after air-lift, the lower part of the keratinocyte region and partly fibroblasts in the gel were immunopositive for TRPV2, although α -SMA immunoreactivity was not observed. After 7 or 9 days, the keratinocyte region was still immunopositive for TRPV2, while immunostaining for TRPV2 and α -SMA was remarkably enhanced in the gel and some of their staining was located in the same cells (Fig. 6). A preliminary test using an anti-S-100 antibody, which

reportedly recognizes preadipocytes, adipocytes, and other types of cells [40], showed considerable immunoreactivity in some cells. These results suggest that some heterogeneous cell populations may be included in this model that will need to be clarified (Suppl. Fig. 1B).

In an immunofluorescence study using excisional cutaneous wounds of 2-day-old rats, TRPV2 was expressed in the newly developed epithelial tongue in association with strong expression of α -SMA in the surrounding granulation tissue (Suppl. Fig. 5), indicating that TRPV2 channels could be a possible target for the inhibition of scar formation.

3.5. TRPV2-mediated increase in intracellular Ca^{2+} levels of TGF- β 1-treated dermal fibroblasts

Since TRPV2 is known to be a Ca^{2+} -permeable channel, an increase of intracellular Ca^{2+} due to TRPV2 activation is expected during the differentiation of fibroblasts. To examine whether TRPV channels were functionally expressed and their actions were sensitive to the inhibitors used in this study, we performed fluorescence measurements of the intracellular Ca^{2+} indicator Fluo-4-AM in rat dermal fibroblasts. The cells were isolated from 2-day-old rats, cultured on glass coverslips, and treated with TGF- β 1 (20 ng/mL) for 48 h (Fig. 7). TGF- β 1 treatment significantly increased the level of α -SMA mRNA relative to that of GAPDH (0 h, 0.91 ± 0.15 ; 48 h, 1.40 ± 0.12 ; $n = 8$, $P < 0.05$, Student's t -test). After pretreatment with TGF- β 1, the TRPV agonist 2-APB (1 mM), the concentration of which has been shown to activate rat TRPV2 fully [22], increased fluorescence intensity in most of the cells and the net increase was approximately 30% of the maximal increase by ionomycin

(Fig. 7A). Without pretreatment with TGF- β 1, however, the net increase in fluorescence by 2-APB was small. Both SKF96365 (30 μ M) and tranilast (30 μ M) significantly inhibited the 2-APB-induced action in the presence of TGF- β 1 (Fig. 7B). After each inhibitor was washed out, the continued presence of 2-APB increased fluorescence intensity drastically. These results suggest that Ca²⁺-permeable TRPV channels were expressed during TGF- β 1 treatment and these effects were effectively inhibited by SKF96365 and tranilast at the concentrations used in the skin equivalent model.

To strengthen the hypothesis that TRPV2 channels are involved in the increase of Ca²⁺ and α -SMA production in TGF- β 1-treated dermal fibroblasts, we silenced TRPV2 expression in these cells using siRNA against TRPV2. Two different TRPV2 siRNA duplexes decreased TRPV2 mRNA levels and inhibited the 2-AP-induced increase of Ca²⁺ as well as α -SMA production (Fig. 8A–C). These observations suggest that the Ca²⁺-permeable channels expressed during TGF- β 1 treatment are mostly TRPV2 channels.

4. Discussion

TGF- β 1 reportedly induces the transition of fibroblasts to their contractile phenotype, that is, myofibroblasts, in various types of tissue [2,6-9]. Although this change in phenotype is important for wound healing, it results in extreme contraction and hypertrophic scar formation. Several mechanisms underlying these phenomena have been reported, though it remains uncertain what type of ion channel is involved in fibroblast differentiation on the basis of interactions between keratinocytes and fibroblasts.

Our present study, using a skin equivalent model, showed that two TRPV2 channel inhibitors, SKF96365 and tranilast, markedly inhibited the contraction of the dermal fibroblast-embedded collagen gel (Fig. 8D): 1) gel contraction and α -SMA production in the skin equivalent were partly mediated by TGF- β type I receptors through the activation of ion channels that can be inhibited by SKF96365 and tranilast; 2) in the absence of keratinocytes, gel contraction was entirely dependent on SKF96365-sensitive Ca²⁺-permeable channels; 3) stratified keratinocytes secreted TGF- β 1 through a mechanism that was decreased by SKF96365 and tranilast; 4) TRPV2 was expressed in keratinocyte layers; and 5) the expression of TRPV2 and TRPV3 was increased in fibroblasts at 5–9 days after the keratinocytes started to stratify. No remarkable or consistent actions were observed for other compounds that are known to activate or inhibit certain types of TRPV channels. Therefore, we considered that TRPV2 may be involved in the contraction of the collagen gel. Tranilast has been used clinically to improve keloid and hypertrophic scars because of its inhibition of collagen accumulation in granulation tissue [26]. Tranilast was shown to inhibit the release of TGF- β 1 from keloid fibroblasts, but not from healthy skin fibroblasts, and to suppress collagen

synthesis in keloid fibroblasts [27]. Thus, inhibition of the possible TRPV candidate, TRPV2, by SKF96365 and tranilast may provide useful approaches to reduce excessive myofibroblast activity and to prevent hypertrophic scarring.

TRP channels are known to contribute to skin biology and pathophysiology [41]. TRPV3 is involved in epidermal wound healing [18], while TRPV4 contributes to epidermal barrier function [19]. Aside from the functional importance of its neuronal expression, TRPV1 channel expression in keratinocytes is upregulated in human skin diseases [41]. In the dermal wound process, TRPC3 and TRPC6 were shown to be expressed in scar tissue and to be involved in Ca^{2+} influx and change of fibroblast phenotype [14,15]. Meanwhile, TRPV2 is known to be a non-selective Ca^{2+} -permeable channel that is activated by noxious heat at temperatures above 52°C [28] and to be most highly expressed in sensory cells and immune cells of the skin [29,41]. However, using real-time RT-PCR and immunofluorescence studies, we found that TRPV2 mRNA and protein were expressed in keratinocyte layers and their expression was increased drastically in fibroblasts after reconstruction was started. Furthermore, we found that Ca^{2+} -permeable TRPV channels were expressed after TGF- β 1 treatment and these effects were effectively inhibited by SKF96365 and tranilast at the concentrations used in the skin model. Although we cannot rule out the possibility that other types of TRP channels, such as TRPC, could be involved in wound contraction, gene silencing using siRNA revealed that TRPV2 channels are likely to contribute significantly to the increase of Ca^{2+} and α -SMA production in the present model. These observations might explain the functional expression of TRPV2 channels during myofibroblast differentiation.

Previously, serum response factor was reported to induce TRPC6 gene expression

downstream of TGF- β -p38 MAPK signaling during myofibroblast differentiation [15]. Several reports also indicated that TGF- β activates serum response factor and induces α -SMA gene expression during myofibroblast differentiation [42,43]. In *in silico* investigations of the rat TRPV2 promoter (-3000 to +1; refGene NM_001270797), we found that there are several putative serum response elements in the proximal region at -301 to -318, -354 to -364, and -611 to -628 using a transcription element search program (JASPAR; <http://jaspar.genereg.net/>). Therefore, the increased level of TGF- β is likely to upregulate TRPV2 and α -SMA mRNA expression during the construction of the skin equivalent model.

Bi-directional regulation between keratinocytes and fibroblasts has been proposed [44]. Myofibroblasts contribute to a hyperproliferative epidermis in human skin equivalents, and *vice versa*, keratinocytes secrete TGF- β 1 and upregulate the expression of α -SMA in fibroblasts near the dermal-epidermal junction [45]. We previously reported the mechanism underlying the effect of keratinocyte-derived TGF- β 1 on myofibroblast differentiation in a rat skin equivalent model [9]: the secretion of latent TGF- β 1 from stratified keratinocytes, the activation of latent TGF- β 1 on the surface of the fibroblasts, and the production of α -SMA through the activation of TGF- β type I receptors. Notably, TGF- β 1 secretion was correlated with the time-dependent contraction of the gel in the present study. TGF- β 1 secretion from keratinocytes for days 3–7 was dependent on TRPV2 channels. In the presence of keratinocytes, the gradually developed phase (days 4–10) of gel contraction was mostly sensitive to TRPV2 and TGF- β receptor inhibitors, while the sudden gel contraction in the earlier phase (days 0–2) was insensitive to them. In the absence of keratinocytes, contraction developed slowly from the beginning without a sudden change, and overall contraction was

inhibited by TRPV2 and TGF- β receptor inhibitors. Therefore, in the skin equivalent model, the later contraction is likely to involve the TRPV2- and TGF- β receptor-mediated action of keratinocytes and fibroblasts, whereas the initial contraction was probably induced by an unidentified keratinocyte-derived growth factor. Other cell-to-cell interactions are likely to account for the keratinocyte-induced differentiation of fibroblasts, such as platelet-derived growth factor and activin, which are reportedly detected in keratinocytes [44]. In the present study, immunoreactivity for S-100 protein was shown to be varied among the cells in the gel (Suppl. Fig. 1B). This raises the questions of how heterogeneous were the fibroblasts that sprouted from rat epidermal tissue in the present isolation procedure and to what extent this putative heterogeneity affects epidermal regeneration and scar contraction ability [40]. These questions remain to be clarified in a future study.

It is becoming apparent that TRP channels play an important role in the response to mechanical stimuli in a wide range of cells [46]. TRPV4- and TRPC3-mediated fibroblast differentiation accompanied with Ca²⁺ influx has been shown to be activated by membrane stretching and matrix stiffness [12,14]. Originally, TRPV2 was described as a noxious heat thermosensor that is activated by chemical reagents, such as 2-APB and cannabinoids [47], but several reports point toward a function for TRPV2 as a mechanosensor in aortic myocytes and neurons [48,49]. Stretch-triggered cation channels were shown to be blocked by the TRPV2 inhibitor tranilast in retinal arterioles [39]. Furthermore, several growth factors (insulin and insulin-like growth factor-1) and serum induced the translocation of TRPV2 from an intracellular compartment to the plasma membrane, which was inhibited by tranilast [23,24]. Therefore, it is possible that the initial gel contraction and growth factors could be triggers to activate TRPV2

channels expressed on fibroblasts and keratinocytes.

In conclusion, this study demonstrated that SKF96365 and tranilast decreased TGF- β 1 release, α -SMA production, and gel contraction of a skin equivalent model. Pharmacological intervention targeting TRPV2 channels during fibroblast differentiation may be beneficial for the prevention of hypertrophic scar formation and contractures.

Acknowledgments

We thank Dr. Makoto Tominaga for his gift of the anti-TRPV2 antibody. We thank Drs. Kennichi Kato and Taiki Suyama for technical assistance and helpful discussions. This work was supported by JSPS KAKENHI (Grant-in-Aid for Scientific Research, Grant Nos. JP15K11358 and JP16K20662) and by MEXT KAKENHI (Grant-in-Aid for Scientific Research on Innovative Areas [Thermal Biology], Grant No. 15H05298). The authors report no conflicts of interest related to this study.

References

- [1] J.M. Rnett, G.S. Ghatnekar, J.A. Palatinus, M. O'Quinn, M.J. Yost, R.G. Gourdie, Novel therapies for scar reduction and regenerative healing of skin wounds, *Trends Biotechnol.* 26 (2008) 173-180.
- [2] J.J. Tomasek, G. Gabbiani, B. Hinz, C. Chaponnier, R.A. Brown, Myofibroblasts and mechano-regulation of connective tissue remodelling. *Nat. Rev. Mol. Cell Biol.* 3 (2002) 349-363.
- [3] I. Darby, O. Skalli, G. Gabbiani, α -Smooth muscle actin is transiently expressed by myofibroblasts during experimental wound healing, *Lab. Invest.* 63 (1990) 21-29.
- [4] S.G. Roy, Y. Nozaki, S.H. Phan, Regulation of α -smooth muscle actin gene expression in myofibroblast differentiation from rat lung fibroblasts, *Int. J. Biochem. Cell Biol.* 33 (2001) 723-734.
- [5] D.J. Abraham, B. Eckes, V. Rajkumar, T. Krieg, New developments in fibroblast and myofibroblast biology: implications for fibrosis and scleroderma, *Curr. Rheumatol. Rep.* 9 (2007) 136-143.
- [6] A. Desmoulière, A. Geinoz, F. Gabbiani, G. Gabbiani, Transforming growth factor- β 1 induces alpha-smooth muscle actin expression in granulation tissue myofibroblasts and in quiescent and growing cultured fibroblasts, *J. Cell Biol.* 122 (1993) 103-111.
- [7] P. Schmid, S. Kunz, N. Cerletti, G. McMaster, D. Cox, Injury induced expression of TGF- β 1 mRNA is enhanced by exogenously applied TGF- β s, *Biochem. Biophys. Res. Commun.* 194 (1993) 399-406.
- [8] L. Yang, T. Chan, J. Demare, T. Iwashina, A. Ghahary, P.G. Scott, E.E. Tredget, Healing of burn wounds in transgenic mice overexpressing transforming growth factor- β 1 in the epidermis, *Am. J. Pathol.* 159 (2001) 2147-2157.

- [9] S. Hata, K. Okamura, M. Hatta, H. Ishikawa, J. Yamazaki, Proteolytic and non-proteolytic activation of keratinocyte-derived latent TGF- β 1 induces fibroblast differentiation in a wound-healing model using rat skin, *J. Pharmacol. Sci.* 124 (2014) 230-243.
- [10] Y. Yang, Z. Wang, H. Yang, L. Wang, S.R. Gillespie, J.M. Wolosin, A.M. Bernstein, P.S. Reinach, TRPV1 potentiates TGF β -induction of corneal myofibroblast development through an oxidative stress-mediated p38-SMAD2 signaling loop, *PLoS One* 8 (2013) e77300.
- [11] R.K. Adapala, R.J. Thoppil, D.J. Luther, S. Paruchuri, J.G. Meszaros, W.M. Chilian, C.K. Thodeti, TRPV4 channels mediate cardiac fibroblast differentiation by integrating mechanical and soluble signals, *J. Mol. Cell. Cardiol.* 54 (2013) 45-52.
- [12] S.O. Rahaman, L.M. Grove, S. Paruchuri, B.D. Southern, S. Abraham, K.A. Niese, R.G. Scheraga, S. Ghosh, C.K. Thodeti, D.X. Zhang, M.M. Moran, W.P. Schilling, D.J. Tschumperlin, M.A. Olman, TRPV4 mediates myofibroblast differentiation and pulmonary fibrosis in mice, *J. Clin. Invest.* 124 (2014) 5225-5238.
- [13] Y. Okada, K. Shirai, P.S. Reinach, A. Kitano-Izutani, M. Miyajima, K.C. Flanders, J.V. Jester, M. Tominaga, S. Saika, TRPA1 is required for TGF- β signaling and its loss blocks inflammatory fibrosis in mouse corneal stroma, *Lab. Invest.* 94 (2014) 1030-1041.
- [14] H. Ishise, B. Larson, Y. Hirata, T. Fujiwara, S. Nishimoto, T. Kubo, K. Matsuda, S. Kanazawa, Y. Sotsuka, K. Fujita, M. Kakibuchi, K. Kawai, Hypertrophic scar contracture is mediated by the TRPC3 mechanical force transducer via NF κ B activation, *Sci. Rep.* 5 (2015) 11620.
- [15] J. Davis, A.R. Burr, G.F. Davis, L. Birnbaumer, J.D. Molkenin, A

- TRPC6-dependent pathway for myofibroblast transdifferentiation and wound healing in vivo, *Dev. Cell* 23 (2012) 705-715.
- [16] L.H. Kurahara, M. Sumiyoshi, K. Aoyagi, K. Hiraishi, K. Nakajima, M. Nakagawa, Y. Hu, R. Inoue, Intestinal myofibroblast TRPC6 channel may contribute to stenotic fibrosis in Crohn's disease, *Inflamm. Bowel Dis.* 21 (2015) 496-506.
- [17] J. Du, J. Xie, Z. Zhang, H. Tsujikawa, D. Fusco, D. Silverman, B. Liang, L. Yue, TRPM7-mediated Ca^{2+} signals confer fibrogenesis in human atrial fibrillation, *Circ. Res.* 106 (2010) 992-1003.
- [18] R. Aijima, B. Wang, T. Takao, H. Mihara, M. Kashio, Y. Ohsaki, J.Q. Zhang, A. Mizuno, M. Suzuki, Y. Yamashita, S. Masuko, M. Goto, M. Tominaga, M.A. Kido, The thermosensitive TRPV3 channel contributes to rapid wound healing in oral epithelia, *FASEB J.* 29 (2015) 182-192.
- [19] T. Sokabe, T. Fukumi-Tominaga, S. Yonemura, A. Mizuno, M. Tominaga, The TRPV4 channel contributes to intercellular junction formation in keratinocytes, *J. Biol. Chem.* 285 (2010) 18749-18758.
- [20] S.B. Amjad, R. Carachi, M. Edward, Keratinocyte regulation of TGF- β and connective tissue growth factor expression: A role in suppression of scar tissue formation, *Wound Repair Regen.* 15 (2007) 748-755.
- [21] J.M. Davidson, Animal models for wound repair, *Arch. Dermatol. Res.* 290 (Suppl) (1998) S1-S11.
- [22] V. Juvin, A. Penna, J. Chemin, Y.L. Lin, F.A. Rassendren, Pharmacological characterization and molecular determinants of the activation of transient receptor potential V2 channel orthologs by 2-aminoethoxydiphenyl borate, *Mol. Pharmacol.* 72 (2007) 1258-1268.

- [23] L. Nie, Y. Oishi, I. Doi, H. Shibata, I. Kojima, Inhibition of proliferation of MCF-7 breast cancer cells by a blocker of Ca²⁺-permeable channel, *Cell Calcium* 22 (1997) 75-82.
- [24] E. Hisanaga, M. Nagasawa, K. Ueki, R.N. Kulkarni, M. Mori, I. Kojima, Regulation of calcium-permeable TRPV2 channel by insulin in pancreatic β -cells, *Diabetes* 58 (2009) 174-184.
- [25] H. Mihara, A. Boudaka, K. Shibasaki, A. Yamanaka, T. Sugiyama, M. Tominaga, Involvement of TRPV2 activation in intestinal movement through nitric oxide production in mice, *J. Neurosci.* 30 (2010) 16536-16544.
- [26] M. Isaji, M. Nakajoh, J. Naito, Selective inhibition of collagen accumulation by N-(3,4-dimethoxycinnamoyl)anthranilic acid (N-5') in granulation tissue, *Biochem. Pharmacol.* 36 (1987) 469-474.
- [27] H. Suzawa, S. Kikuchi, N. Arai, A. Koda, The mechanism involved in the inhibitory action of tranilast on collagen biosynthesis of keloid fibroblasts, *Jpn. J. Pharmacol.* 60 (1992) 91-96.
- [28] M.J. Caterina, T.A. Rosen, M. Tominaga, A.J. Brake, D. Julius, A capsaicin-receptor homologue with a high threshold for noxious heat, *Nature* 398 (1999) 436-441.
- [29] A. Perálvarez-Marín, P. Doñate-Macian, R. Gaudet, What do we know about the transient receptor potential vanilloid 2 (TRPV2) ion channel? *FEBS J.* 280 (2013) 5471-5487.
- [30] K. Shibasaki, Physiological significance of TRPV2 as a mechanosensor, thermosensor and lipid sensor, *J. Physiol. Sci.* 66 (2016) 359-365.
- [31] W. Sun, K. Uchida, N. Takahashi, Y. Iwata, S. Wakabayashi, T. Goto, T. Kawada, M. Tominaga, Activation of TRPV2 negatively regulates the differentiation of mouse

- brown adipocytes, *Pfluger's Arch.* 468 (2016) 1527-1540.
- [32] S. Hassan, K. Eldeeb, P.J. Millns, A.J. Bennett, S.P. Alexander, D.A. Kendall, Cannabidiol enhances microglial phagocytosis via transient receptor potential (TRP) channel activation, *Br. J. Pharmacol.* 171 (2014) 2426-2439.
- [33] I. Pottosin, I. Delgado-Enciso, E. Bonales-Alatorre, M.G. Nieto-Pescador, E.G. Moreno-Galindo, O. Dobrovinskaya, Mechanosensitive Ca²⁺-permeable channels in human leukemic cells: pharmacological and molecular evidence for TRPV2, *Biochim. Biophys. Acta.* 1848 (2015) 51-59.
- [34] L. Gao, P. Yang, P. Qin, Y. Lu, X. Li, Q. Tian, Y. Li, C. Xie, J.B. Tian, C. Zhang, C. Tian, M.X. Zhu, J. Yao, Selective potentiation of 2-APB-induced activation of TRPV1-3 channels by acid, *Sci. Rep.* 6 (2016) 20791.
- [35] F. Zhang, H. Yang, Z. Wang, S. Mergler, H. Liu, T. Kawakita, S.D. Tachado, Z. Pan, J.E. Capó-Aponte, U. Pleyer, H. Koziel, W.W. Kao, P.S. Reinach, Transient receptor potential vanilloid 1 activation induces inflammatory cytokine release in corneal epithelium through MAPK signaling, *J. Cell. Physiol.* 213 (2007) 730-739.
- [36] C.H. Feetham, N. Nunn, R. Lewis, C. Dart, R. Barrett-Jolley, TRPV4 and K_{Ca} ion channels functionally couple as osmosensors in the paraventricular nucleus, *Br. J. Pharmacol.* 172 (2015) 1753-1768.
- [37] K. Narita, S. Sasamoto, S. Koizumi, S. Okazaki, H. Nakamura, T. Inoue, S. Takeda, TRPV4 regulates the integrity of the blood-cerebrospinal fluid barrier and modulates transepithelial protein transport, *FASEB J.* 29 (2015) 2247-2259.
- [38] H. Che, G.S. Xiao, H.Y. Sun, Y. Wang, G.R. Li, Functional TRPV2 and TRPV4 channels in human cardiac c-kit⁺ progenitor cells, *J. Cell. Mol. Med.* 20 (2016) 1118-1127.

- [39] M.K. McGahon, J.A. Fernández, D.P. Dash, J. McKee, D.A. Simpson, A.V. Zholos, J.G. McGeown, T.M. Curtis, TRPV2 Channels Contribute to Stretch-Activated Cation Currents and Myogenic Constriction in Retinal Arterioles, *Invest. Ophthalmol. Vis. Sci.* 57 (2016) 5637-5647.
- [40] S. Aoki, S. Toda, T. Ando, H. Sugihara, Bone marrow stromal cells, preadipocytes, and dermal fibroblasts promote epidermal regeneration in their distinctive fashions, *Mol. Biol. Cell.* 15 (2004) 4647-4657.
- [41] M.J. Caterina, Z. Pang, TRP Channels in Skin Biology and Pathophysiology, *Pharmaceuticals* 9 (2016) 77.
- [42] J. Chai, M. Norng, A.S. Tarnawski, J. Chow, A critical role of serum response factor in myofibroblast differentiation during experimental oesophageal ulcer healing in rats, *Gut* 56 (2007) 621-630.
- [43] N. Sandbo, S. Kregel, S. Taurin, S. Bhorade, N.O. Dulin, Critical role of serum response factor in pulmonary myofibroblast differentiation induced by TGF- β , *Am. J. Respir. Cell Mol. Biol.* 41 (2009) 332-338.
- [44] S. Werner, T. Krieg, H. Smola, Keratinocyte-fibroblast interactions in wound healing, *J. Invest. Dermatol.* 127 (2007) 998-1008.
- [45] L. Yang, K. Hashimoto, M. Tohyama, H. Okazaki, X. Dai, Y. Hanakawa, K. Sayama, Y. Shirakata, Interactions between myofibroblast differentiation and epidermogenesis in constructing human living skin equivalents, *J. Dermatol. Sci.* 65 (2012) 50-57.
- [46] S.F. Petersen, B. Nilius, Transient receptor potential channels in mechanosensing and cell volume regulation, in: D. Häussinger and H. Sies (Eds.), *Methods in Enzymology* 428 Osmosensing and Osmosignaling, Elsevier Inc., Netherlands, 2007,

pp. 183-207.

- [47] J. Vriens, G. Appendino, B. Nilius, Pharmacology of vanilloid transient receptor potential cation channels, *Mol. Pharmacol.* 75 (2009) 1262-1279.
- [48] K. Muraki, Y. Iwata, Y. Katanosaka, T. Ito, S. Ohya, M. Shigekawa, Y. Imaizumi, TRPV2 is a component of osmotically sensitive cation channels in murine aortic myocytes, *Circ. Res.* 93 (2003) 829-838.
- [49] K. Shibasaki, N. Murayama, K. Ono, Y. Ishizaki, M. Tominaga, TRPV2 enhances axon outgrowth through its activation by membrane stretch in developing sensory and motor neurons, *J. Neurosci.* 30 (2010) 4601-4612.

Figure legends

Fig. 1. Schematic diagram for the model of rat skin and dependency of collagen gel contraction on keratinocytes (KC) in the presence or absence of TGF- β 1 (40 ng/mL) or LY364947 (3 μ M). A, The collagen gel surface was transferred to the air-liquid interface (air-lift) to induce stratification of the keratinocytes. The area of the gel was divided by the effective membrane area of the culture insert to obtain the relative gel size at each time point (% of the initial gel size). B, In the KC(+) group, keratinocytes were seeded on the surface of the collagen gel on day 0, and the air-lift was performed on the next day. In the KC(-) group, the gel surface without keratinocytes was transferred to the air-liquid interface on day 1. In some preparations, keratinocytes were seeded on a gel that contained no fibroblasts (KC w/o fibroblasts). Each compound was added to the culture medium on day 0. Gel size was measured with an image analyzer and expressed as % of the initial size (n = 3). C, % of contraction on day 10 in the presence or absence of TGF- β 1 or LY364947. * P < 0.05, *** P < 0.001 vs. the corresponding control group. Some standard error bars are hidden by the marks. The dashed line indicates the level of the control in the KC(+) group.

Fig. 2. Effects of several TRP channel activators and inhibitors on collagen gel contraction in the presence (KC[+], n = 6) or absence (KC[-], n = 3) of keratinocytes. Each compound was added to the culture medium on day 0. A, Time course of collagen gel contraction. Gel size is expressed as % of the initial size (n = 3). Standard error bars are hidden in the marks. B, % of contraction on day 10 in the presence of TRP channel activators and inhibitors. ** P < 0.01, *** P < 0.001 vs. the corresponding control group.

Fig. 3. Effects of the TRPV2 inhibitors SKF96365 and tranilast in the rat skin models. A, Time course of collagen gel contraction in the presence of keratinocytes. Gel size is expressed as % of the initial size ($n = 3$). Some standard error bars are hidden by the marks. B, Concentration-dependent inhibition of gel contraction induced by these compounds at 10 days after the keratinocytes were seeded. Differences of gel size in the presence of SKF96365 or tranilast at each concentration from that in their absence are shown ($n = 3$). Data were fitted to sigmoidal curves. IC_{50} values were $19.6 \pm 0.7 \mu\text{M}$ for SKF96365 ($n = 3$, slope = 0.089, $R^2 = 0.998$) and $17.7 \pm 1.6 \mu\text{M}$ for tranilast ($n = 3$, slope = 0.085, $R^2 = 0.996$). C, Concentration-dependent inhibition of α -SMA mRNA levels induced by these compounds at 8 days after the keratinocytes were seeded ($n = 3$). D, Keratinocyte-induced release of TGF- β 1 into the culture supernatant in the presence or absence of SKF96365 (50 μM) and tranilast (75 μM). Culture supernatant was collected during days 3–7 after the epithelial cells were seeded on the collagen gel without fibroblasts. The culture media were free of serum. $***P < 0.001$ ($n = 4$).

Fig. 4. Effects of the TRPV2 inhibitors SKF96365 and tranilast on the TGF- β 1-mediated contraction of the KC(-) models. LY364947 was added to examine the involvement of the TGF- β pathway in the actions of SKF96365 and tranilast on contraction. A, Time course of collagen gel contraction. Gel size is expressed as % of the initial size ($n = 3$). Standard error bars are hidden by the marks. B, % of contraction on day 10 in the presence or absence of TRP channel inhibitors and LY364947. Broken line shows the level of contraction without the compounds. $***P < 0.001$ vs. the TGF- β 1 group. $####P < 0.001$ vs. the TGF- β 1 + LY364947 group.

Fig. 5. Quantitative comparison of mRNA levels of TRPV channels and α -SMA in fibroblasts embedded in the collagen gel and in stratified keratinocytes at 5, 7, and 9 days after air-lift (real-time PCR). Dermal (D) and epidermal (E) tissues obtained from 2-day-old rats were also compared. The mRNA levels are normalized to the GAPDH values ($n = 3-4$).

Fig. 6. Immunofluorescence assessments of *in vivo* rat skin and the 3D reconstruction model at 5, 7, and 9 days after air-lift. Green: TRPV2; red: α -SMA. Broken line indicates the border line between the keratinocyte layers and the collagen gel. Dotted line indicates the surface of the keratinocytes. The merged immunopositive cells are indicated by arrowheads. Nuclei were counterstained (DAPI).

Fig. 7. Intracellular Ca^{2+} imaging. A, Time course of the mean intensity of fluorescence emitted from dermal fibroblasts in 3 different images. Fibroblasts were obtained from 2-day-old rats and pretreated with or without TGF- β 1 (40 ng/mL) for 48 h. The cells were loaded with the Ca^{2+} indicator Fluo-4-AM prior to the experiments. 2-APB (1 mM) was perfused in the presence or absence of SKF96365 (30 μM) or tranilast (30 μM). Fluorescence intensity (%) was normalized with the maximal value obtained in the presence of ionomycin (5 μM). B, Summarized data for the increases in 2-APB-induced fluorescence obtained in the various conditions. Data are expressed as the summation of relative intensity for 30 s from the beginning of 2-APB application in the presence or absence of each inhibitor. * $P < 0.01$ ($n = 3$).

Fig. 8. Intracellular Ca^{2+} imaging data using TRPV2 siRNA and a schematic model of

this study. A, Time course of the mean intensity of fluorescence emitted from dermal fibroblasts in 3 different images. Rat fibroblasts were transfected with a negative control or TRPV2 siRNA (#1 or #2) and pretreated with TGF- β 1 (40 ng/mL) for 48 h. The cells were loaded with the Ca²⁺ indicator Fluo-4-AM prior to the experiments. 2-APB (1 mM) was perfused and fluorescence was measured. Intensity (%) was normalized with the maximal value obtained in the presence of ionomycin (5 μ M). B, Summarized data for the increases in 2-APB-induced fluorescence in the fibroblasts transfected with the control or TRPV2 siRNA (#1 or #2). Data are expressed as the summation of relative intensity during 2-APB application (45 s). * $P < 0.05$, *** $P < 0.001$ (n = 3) vs. the corresponding control RNA. D, Schematic model of pharmacological blockade by TRP inhibitors during fibroblast differentiation and contraction mediated by keratinocyte (KC)-derived TGF- β 1 in the wound healing model of rats.

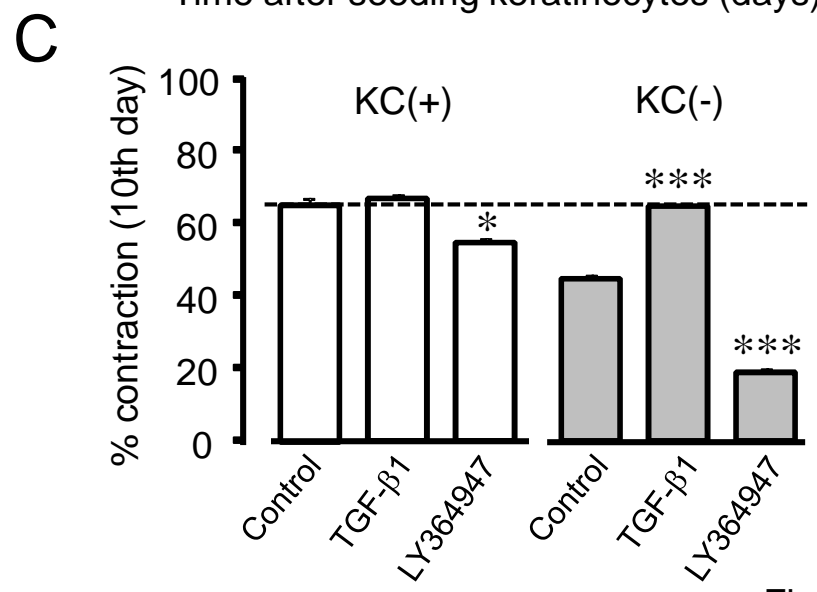
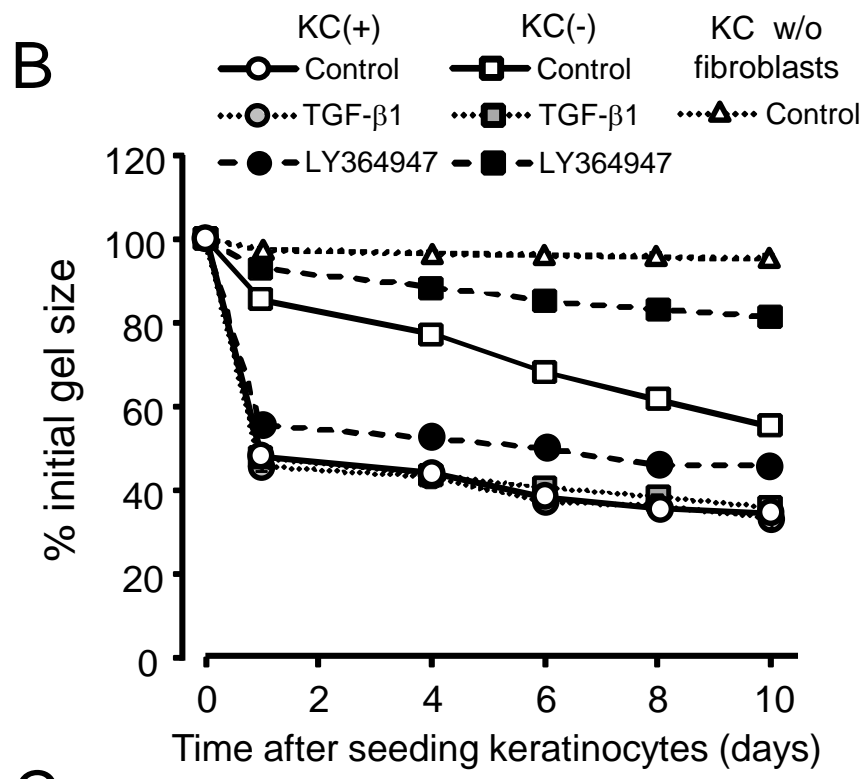
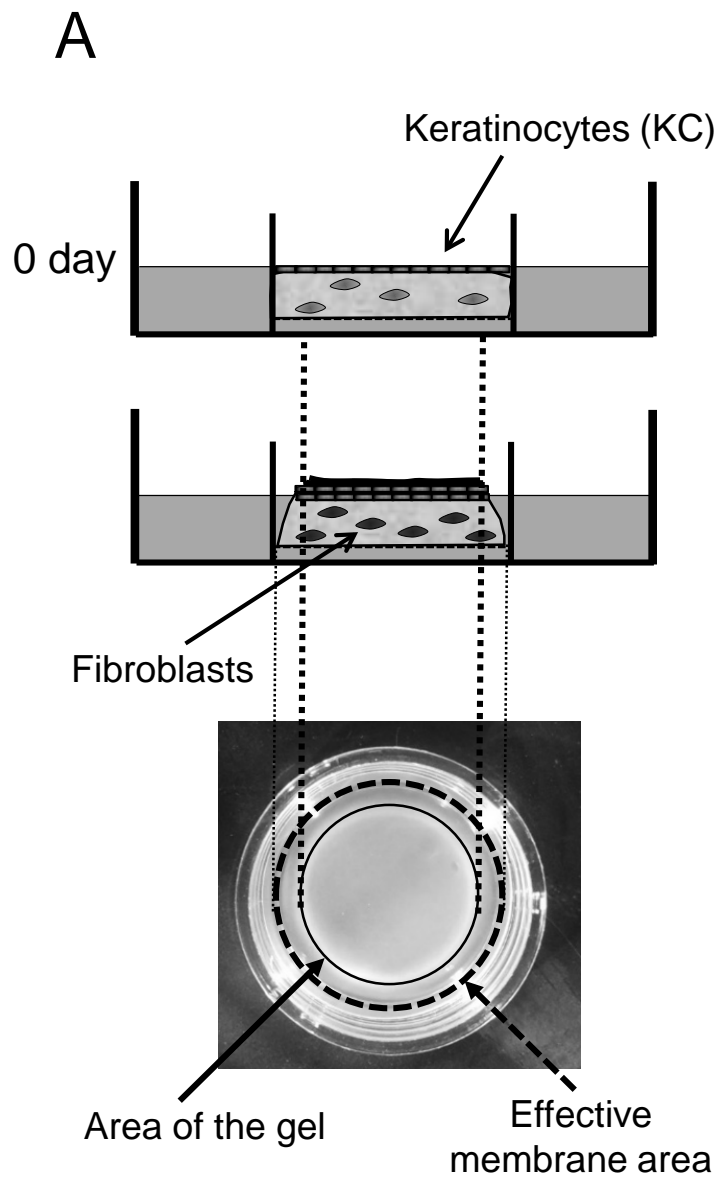
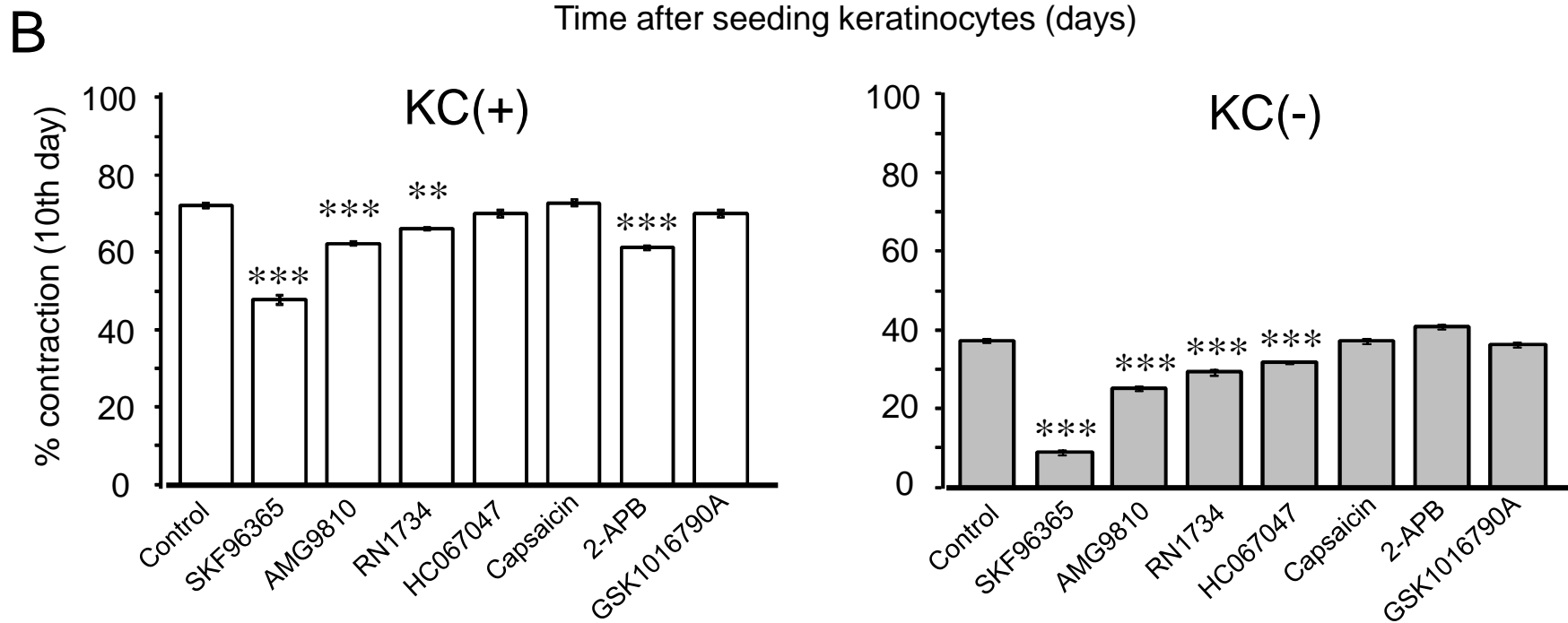
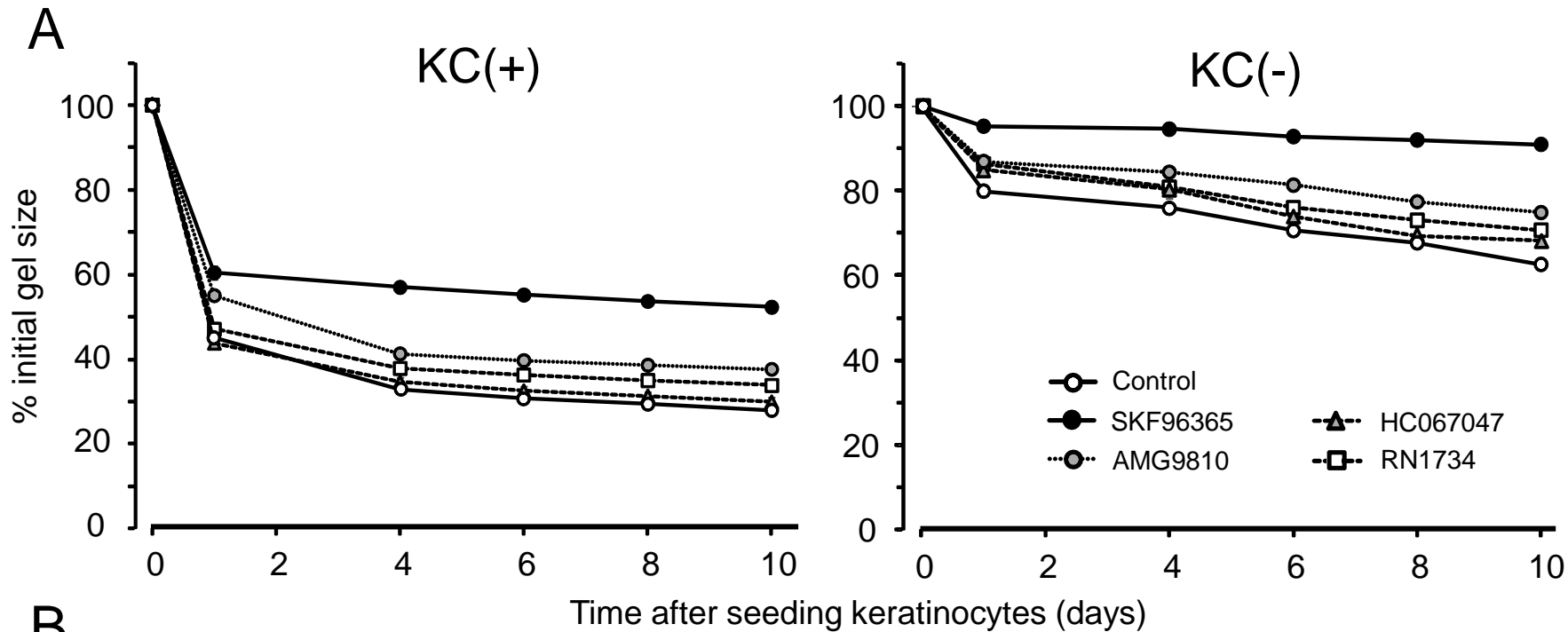


Fig.1 Ishii et al.



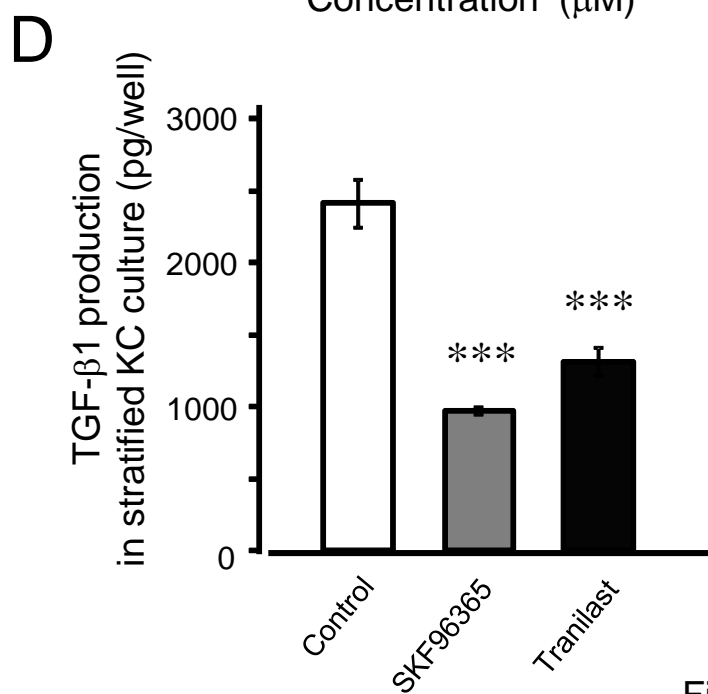
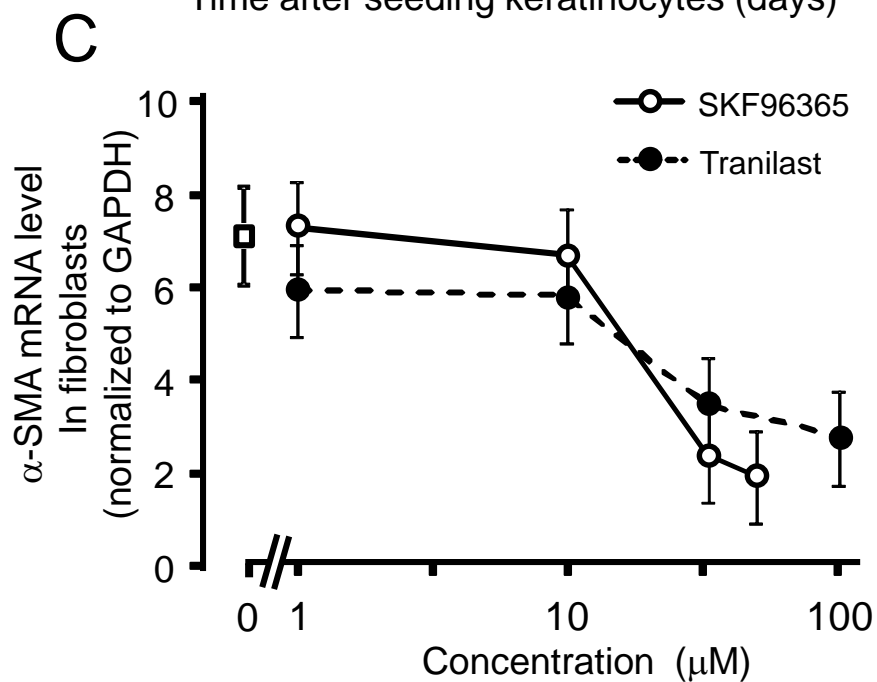
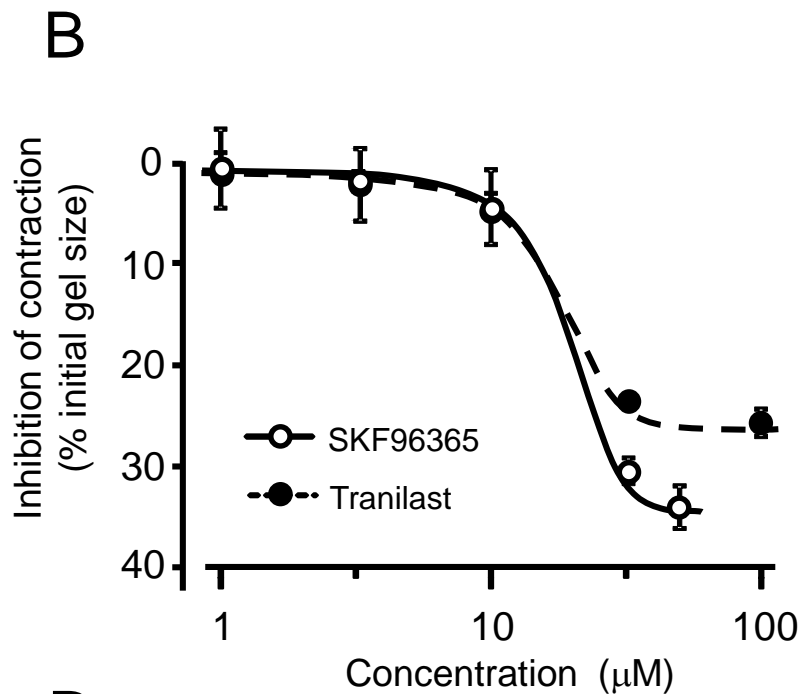
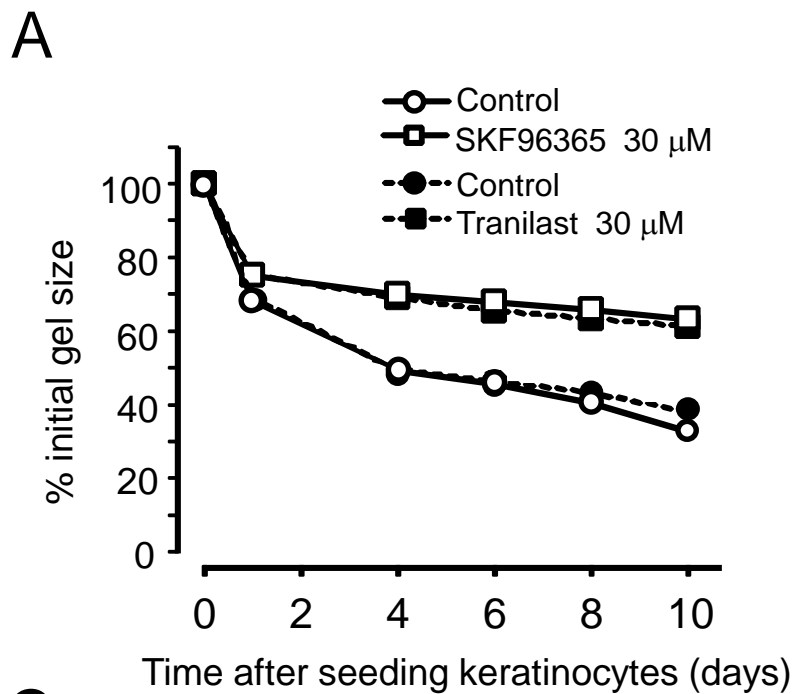
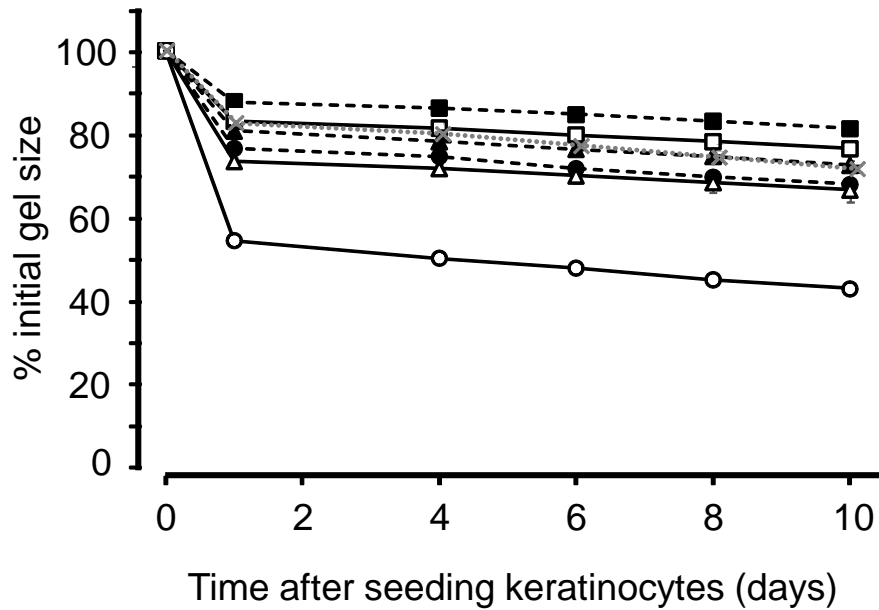


Fig.3 Ishii et al.

A

- ×·· Control
- TGF-β1
- TGF-β1 + SKF96365
- △ TGF-β1 + Tranilast
- TGF-β1 + LY364947
- TGF-β1 + SKF96365 + LY364947
- ▲ TGF-β1 + Tranilast + LY364947



B

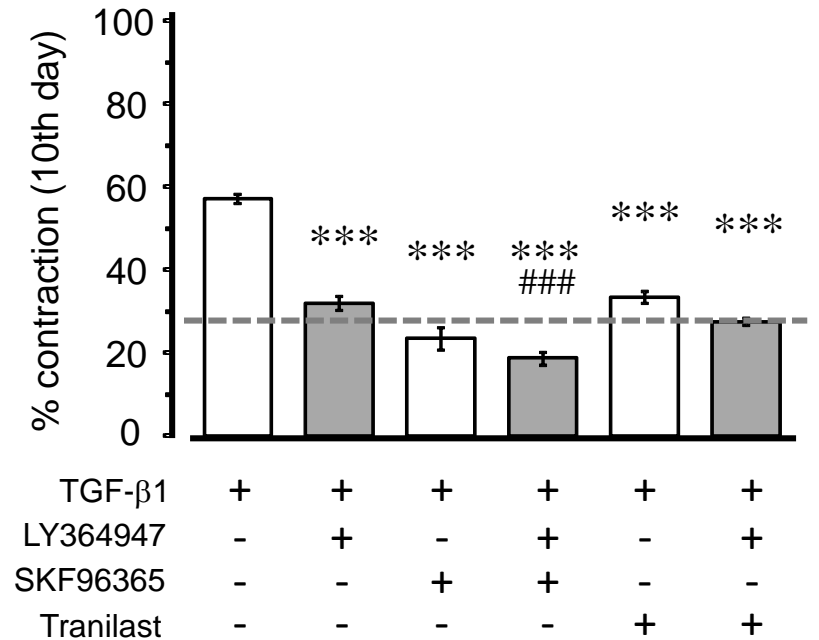


Fig.4 Ishii et al.

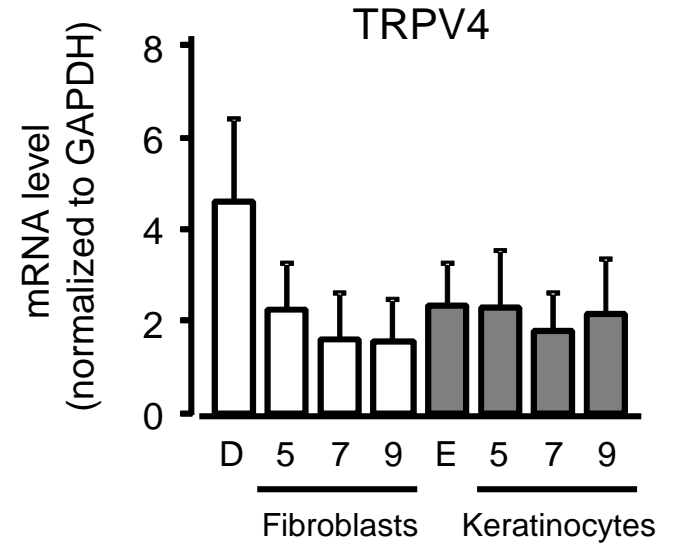
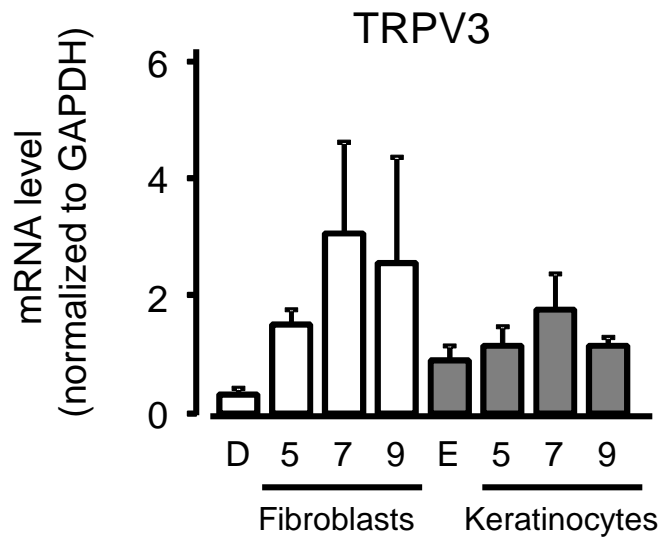
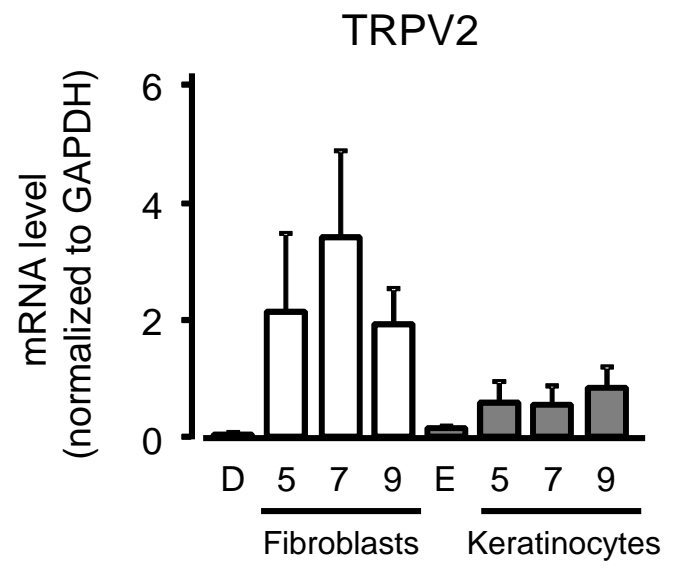
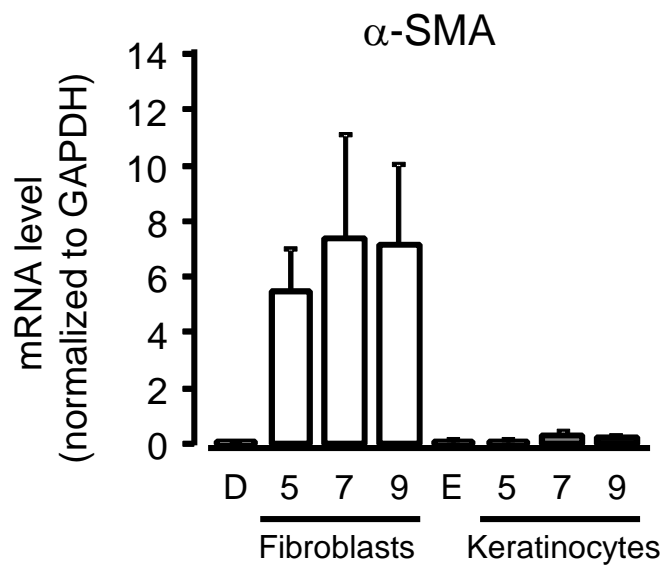
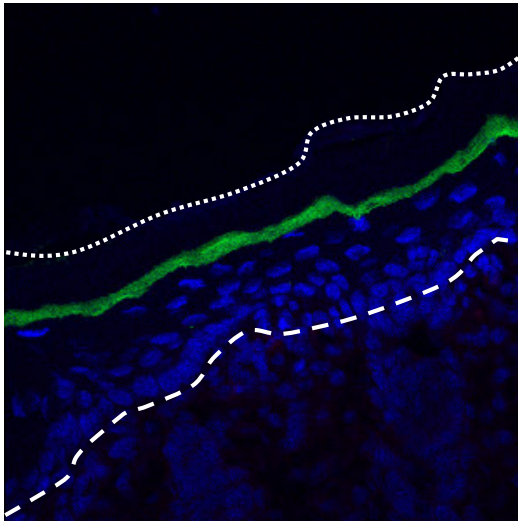
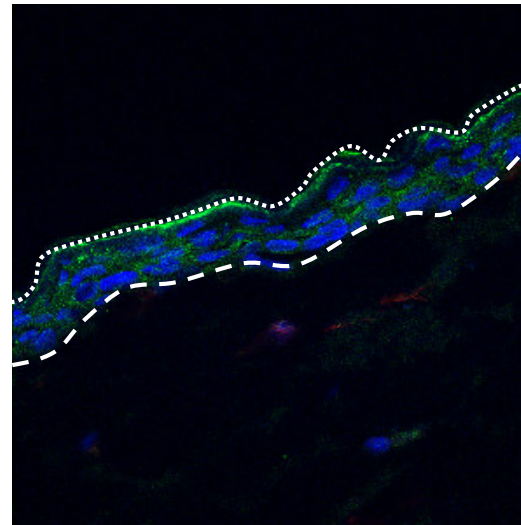


Fig.5 Ishii et al.

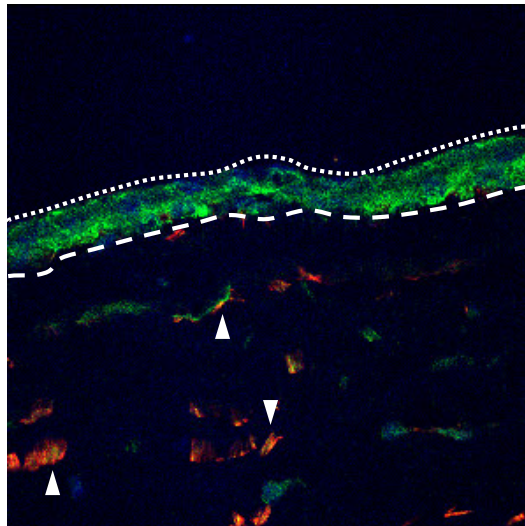
Skin



5 days



7 days



9 days

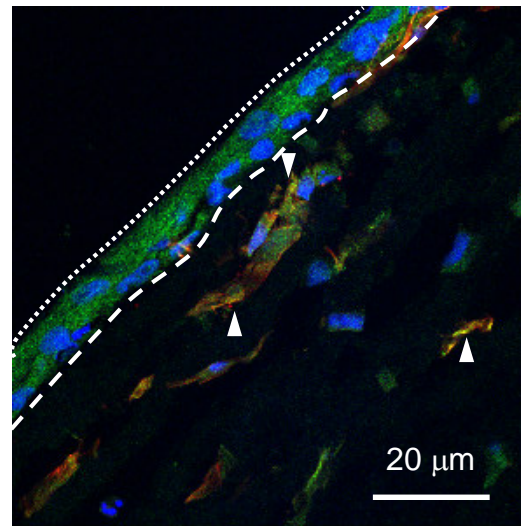


Fig.6 Ishii et al.

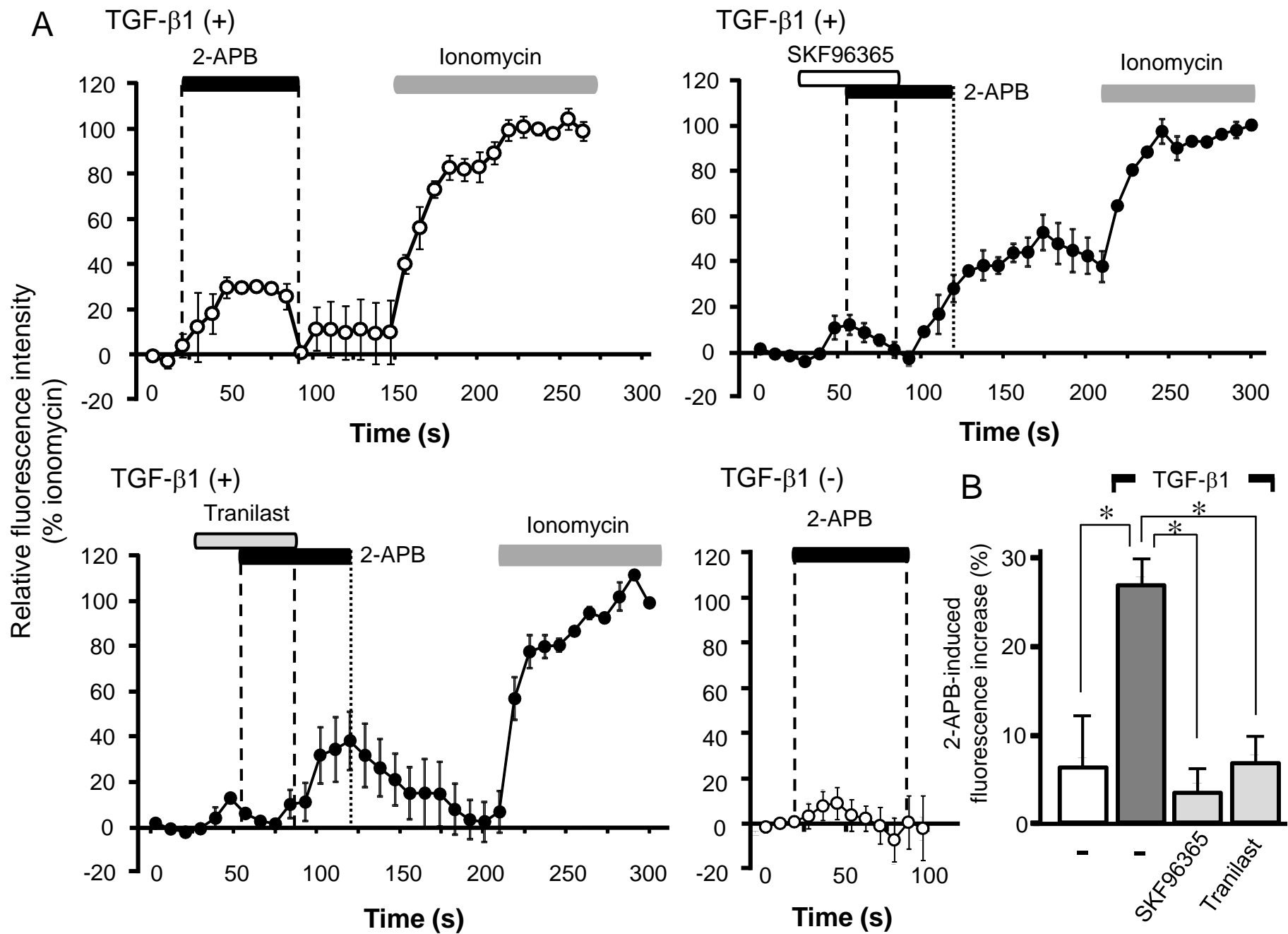


Fig.7 Ishii et al.

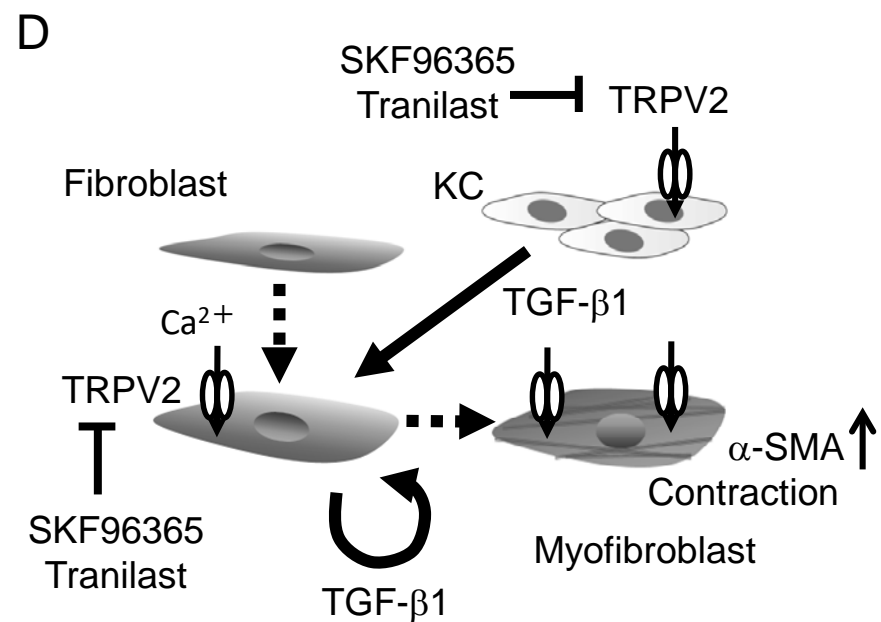
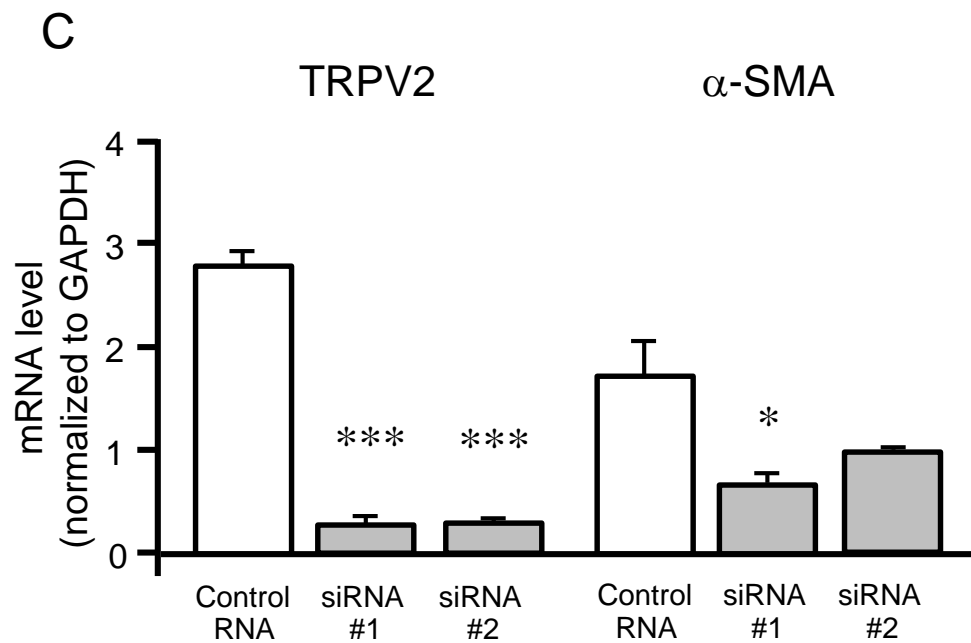
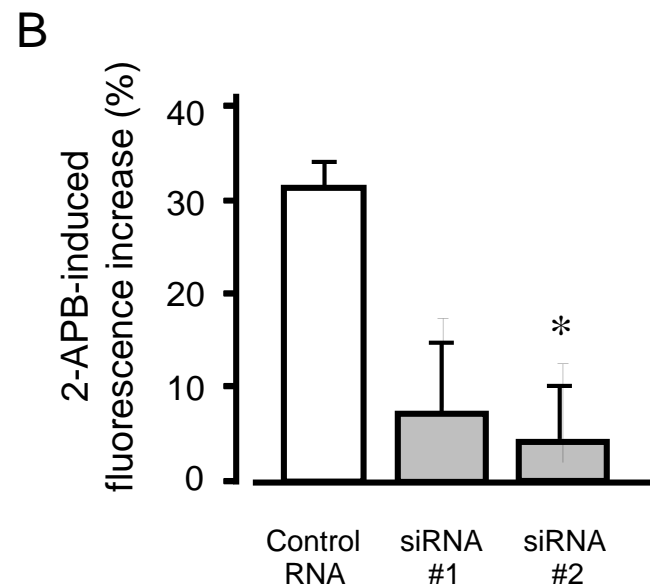
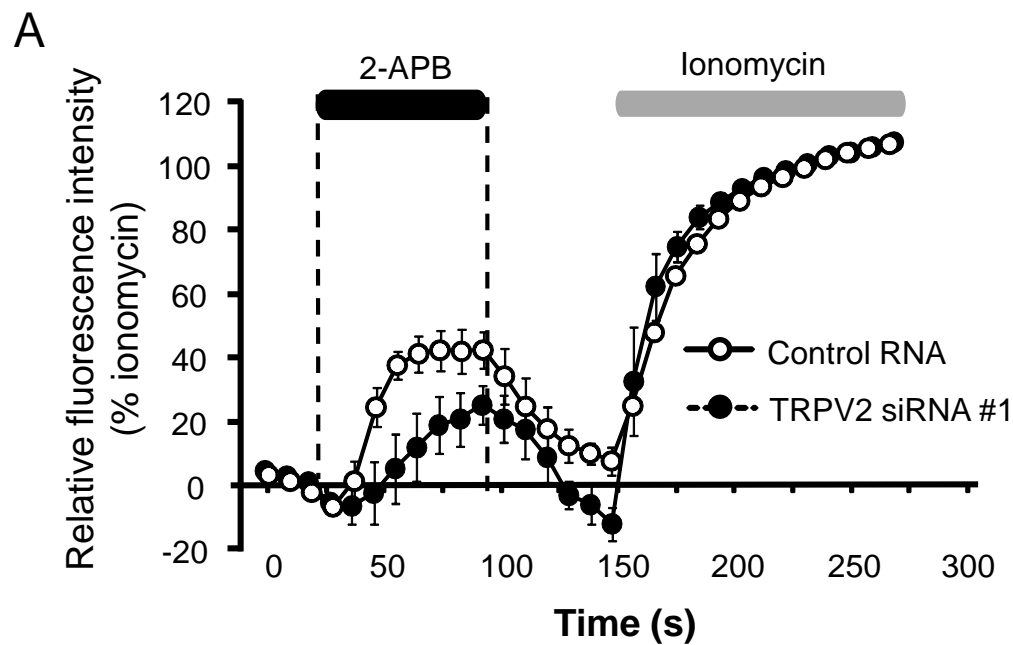


Fig.8 Ishii et al.